Binding of Distamycin A and Netropsin to the 12mer DNA Duplexes Containing Mixed AT·GC Sequences with At Most Five or Three Successive AT Base Pairs†

Jurij Lah and Gorazd Vesnaver*

Department of Chemistry, University of Ljubljana, Aškerčeva 5, 1000 Ljubljana, Slovenia

Received April 3, 2000; Revised Manuscript Received May 22, 2000

ABSTRACT: Circular dichroism (CD), isothermal calorimetric titrations (ITC), and temperature-dependent UV spectroscopy were used to investigate binding of the minor groove-directed ligands distamycin A (Dst) and netropsin (Net) to the following duplexes: d(GTTAGTATTTGG)·d(CCAAATACTAAC), d(GTTAGTATATGG)·d(CCATATACTAAC), d(GTTAGTACTTGG)·d(CCAAGTACTAAC), and d(GTTAGTAGTTGG)·d(CCAACTACTAAC). Our results reveal that Dst binds within the minor grooves of these dodecamers that contain five-AT and/or four-AT·GC binding sites exclusively in a dimeric high-affinity 2:1 binding mode ($K \approx 10^{16}$ M^{-2}). By contrast, Net exhibits high-affinity binding only when it binds in a 1:1 mode ($K_1 \approx 10^9$ M^{-1}) to the two duplexes that contain five-AT sites (5′-TATTT-3′ and 5′-TATAT-3′). Its further binding to these two duplexes occurs in a low-affinity mode ($K_2 \approx 10^6$ M^{-1}) and results in the formation of 2:1 Net−DNA complexes. To the other two duplexes that contain sequences with at most three AT consecutive base pairs Net binds in two distinctive low-affinity 1:1 binding modes ($K_1 \approx 10^7$ M^{-1}, $K_2 \approx 10^6$ M^{-1}). Competition experiments (CD and ITC titrations) reveal that Dst entirely displaces Net from its 1:1 and 2:1 complexes with any of the four duplexes. We discuss and interpret our optical and calorimetric results in the context of the available structural information about the complexes between DNA and the sequence-specific minor groove binders Dst and Net.

Monocationic distamycin A (Dst)[1] and dicationic netropsin (Net) are natural oligopeptides whose pharmacological activities have been correlated to their ability to bind preferentially to the AT-rich domains in the minor groove of DNA (*1*−*4*). The complexes formed between the two drugs and various DNA oligomers and polymers have been used as model systems for the investigation of the sequence-specific recognition of DNA by proteins and small molecules and have thus been the subject of numerous studies. Several such studies have revealed that Dst and Net molecules are able to penetrate deep into the minor groove of DNA where, spanning at least four AT base pairs, they are stabilized in a form of 1:1 complexes by a combination of hydrogen bonding, van der Waals contacts, and electrostatic interactions (*2*, *5*−*8*). It has also been shown that such 1:1 binding of Dst and Net to sequences containing GC base pairs is hindered due to the steric clash between the pyrrole H3 protons of the ligands and the guanidine amino group at the floor of the minor groove (*5*).

Several recent studies on Dst−DNA and Net−DNA complexes have shown that two Dst molecules can bind simultaneously to the minor groove of the sequence that contains at least five successive AT base pairs (*9*−*15*). In such 2:1 complexes, two ligands are stacked side-by-side in a head-to-tail orientation. It has been further shown that the preference for the 2:1 binding mode over the 1:1 mode depends strongly on the DNA sequence. In five-AT base pair sequences characterized by a narrow minor groove, the 1:1 binding is favored, while in those with a wider or more flexible minor groove, the 2:1 motif prevails (*16*). Consistent with this interpretation of the dimeric Dst−DNA complexation is also the observed highly cooperative 2:1 binding of Dst to 4AT·GC sites (*11*). Apparently, the replacement of an AT base pair by a single GC base pair locally widens the minor groove which therefore requires the second Dst molecule in the form of a 2:1 complex for tight contacts with its wall. In contrast to Dst, the doubly charged Net binds within the minor groove of the favorable four-AT or five-AT sites always in a 1:1 high-affinity mode. Evidently, electrostatic repulsion between the charged ends of Net molecules prevents their side-by-side arrangements in the minor groove (*5*). According to numerous studies on ligand binding to DNA, there is probably no simple general code that explains the binding affinity and specificity of minor groove ligands. However, these studies do show that the sequence-dependent variations in the minor groove geometry and/or flexibility play an important role in determining the formation of both 1:1 and 2:1 complexes (*15*). It is generally believed that a better understanding of factors which govern the formation of such complexes will be of great value in designing new drugs that would show optimum affinity and specificity for specific sequence targets within DNA molecules.

† This work was partially supported by the U.S.-Slovene Science and Technology Joint Fund through the following grant: Drug-DNA binding thermodynamics.

* To whom correspondence should be addressed: Department of Chemistry, University of Ljubljana, Aškerčeva 5, 1000 Ljubljana, Slovenia. Fax: +38661 1254458. E-mail: gorazd.vesnaver@uni-lj.si.

[1] Abbreviations: Dst, distamycin A; Net, netropsin; oligomeric DNA duplexes D#1−D#4, d(GTTAGTATTTGG)·d(CCAAATACTAAC), d(GTTAGTATATGG)·d(CCATATACTAAC), d(GTTAGTACTTGG)·d(CCAAGTACTAAC), and d(GTTAGTAGTTGG)·d(CCAACTACTAAC), respectively; CD, circular dichroism; DSC, differential scanning calorimetry; ITC, isothermal titration calorimetry.

10.1021/bi000748u CCC: $19.00
Published on Web 07/08/2000

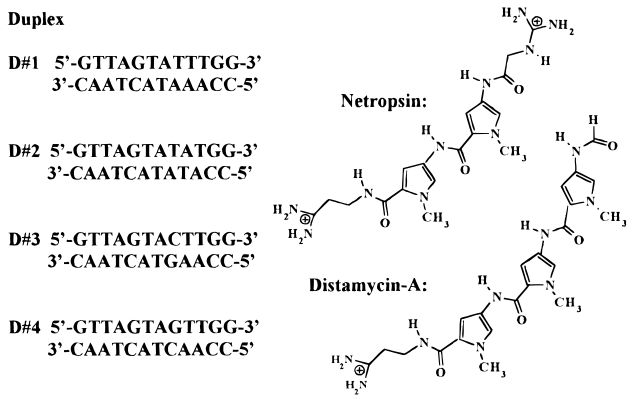

FIGURE 1: Structure of the ligands netropsin (Net) and distamycin A (Dst) and sequences of dodecameric duplexes denoted as D#1−D#4 to which binding of Dst and Net was studied.

In this work, spectroscopic (UV and CD) and calorimetric (DSC and ITC) techniques were used to study the affinity and specificity of Dst and Net binding to the four dodecamers containing different AT·GC sequences. We present here a full thermodynamic description of Dst and Net binding to duplexes d(GTTAGTATTTGG)·d(CCAAATACTAAC), d(GTTAGTATATGG)·d(CCATATACTAAC), d(GTTAGTACTTGG)·d(CCAAGTACTAAC), and d(GTTAGTAGTTGG)·d(CCAACTACTAAC) (termed the D#1−D#4 duplexes hereafter; see Figure 1). Our results demonstrate that to five-AT or four-AT·GC sites contained by the four 12mers Dst binds exclusively in a dimeric high-affinity 2:1 binding mode. On the other hand, Net shows high-affinity 1:1 binding only to five-AT sites contained in duplexes D#1 and D#2, while to duplexes D#3 and D#4 that contain at most three consecutive AT base pairs it binds in a low-affinity 1:1 mode. We were also able to show that upon addition of Net to any of the four 1:1 Net−DNA complexes (high affinity with D#1 and D#2 or low affinity with D#3 and D#4) low-affinity binding of the second Net molecule occurs at the unoccupied ends of the duplex molecules, resulting in the formation of the corresponding 2:1 complexes. According to our competition studies (ITC and CD titrations), Dst entirely displaces Net from its 1:1 and 2:1 complexes with any of the four duplexes. This result is consistent with the thermodynamic binding profiles determined for both ligands which show that for each of the measured dodecamers Dst has significantly higher overall binding affinity than Net.

MATERIALS AND METHODS

Oligonucleotides. The DNA dodecameric duplexes presented in Figure 1 were prepared from the corresponding single strands that were synthesized using the standard cyanoethylphosphoramide chemistry (*18*). The molar extinction coefficients of the single-stranded oligomers were determined by phosphate analysis as described by Griswold et al. (*19*). Duplexes D#1−D#4 (Figure 1) were obtained by mixing the appropriate single strands in a 1:1 molar ratio. Their extinction coefficients determined in 10 mM sodium cacodylate buffer at 260 nm and 25 °C from the corresponding Job plots (*20*) are 168 000, 165 000, 172 000, and 162 000 M^{-1} cm^{-1} for D#1−D#4, respectively.

Drugs. Netropsin-HCl (Net) from Boehringer Mannheim GmbH and distamycin A-HCl (Dst) from Sigma (Figure 1) were used without further purification. Their concentrations

Table 1: Binding Constants K_1, K_2, and K ($=K_1K_2$) for Net Binding to the First, Second, and Both Binding Sites of Duplexes D#1−D#4 in the 10 mM Sodium Cacodylate Buffer Solutions Determined from the CD Titration Curves at 275 nm and 20 °C[a]

duplex	K_1 (M^{-1})	K_2 (M^{-1})	K ($=K_1K_2$) (M^{-2})
D#1	$(4 \pm 1) \times 10^9$	$(3.8 \pm 0.6) \times 10^6$	1.4×10^{16}
D#2	$(2 \pm 1) \times 10^9$	$(6.5 \pm 0.5) \times 10^6$	1.6×10^{16}
D#3	$(5 \pm 2) \times 10^6$	$(5 \pm 2) \times 10^6$	2.5×10^{13}
D#4	$(2 \pm 2) \times 10^7$	$(2 \pm 2) \times 10^7$	4.0×10^{14}

[a] When the χ^2 fitting procedure was performed, a relative error of ±5% was taken for each experimental point.

in solutions were determined spectrophotometrically at 25 °C using the following extinction coefficients: Net, $\epsilon_{296} = 21\,500$ M^{-1} cm^{-1}; and Dst, $\epsilon_{303} = 34\,000$ M^{-1} cm^{-1}. Unless otherwise stated, the buffer solution used in our experiments consisted of 10 mM sodium cacodylate, 100 mM NaCl, and 1 mM Na_2EDTA adjusted to pH 6.9. In this buffer solution, Net and Dst obey Beer's law below 1.5 and 0.9 mM, respectively, which implies that below these concentrations Net and Dst do not show any noticeable association.

Differential Scanning Calorimetry (DSC). The excess heat capacity, $\langle C_p \rangle$, versus temperature profiles for the thermally induced transitions of the four drug-free DNA duplexes were determined using a Nano-DSC differential scanning calorimeter (CSC, Provo, UT). Transition enthalpies, ΔH_{cal}, were calculated from the area under the $\langle C_p \rangle$ versus T curves using ORIGIN version 4.1 software (Microcal, Northampton, MA). The heating rate was 1 °C/min, and the DNA solutions were 100 μM in duplex. The helix to coil transition enthalpies, ΔH_{DSC}, of the four duplexes obtained directly from the measured DSC thermograms (Table 2) range between 90 and 96 kcal/mol per duplex and agree well with the corresponding van't Hoff values of 85−87 kcal/mol of duplex obtained from the slopes of the UV melting curves at T_m (not shown here). Furthermore, they also agree well with the van't Hoff enthalpies of 88.0 and 87.3 kcal/mol of duplex obtained for D#4 in 100 and 50 mM NaCl from the corresponding $1/T_m$ versus ln c_T plots (*21*) (not shown here). Taken together, these results indicate that the temperature-induced helix to coil transition of each of the 12mer duplexes may be considered as a two-state transition characterized by the enthalpy of transition that does not depend on the added salt concentration (between 50 and 100 mM NaCl).

UV Absorption Spectrophotometry. To access the effect of the bound Net or Dst on the thermal stability of the four duplexes, UV melting experiments were conducted in the absence and presence of each ligand. Absorbance versus temperature profiles were measured in the Cary 1 UV spectrophotometer (Varian) equipped with a thermoelectrically controlled cell holder at 260 nm and a heating rate of 0.5 °C/min. The concentration of each 12mer duplex was 5 μM, while the Net and Dst concentrations varied from 0 to 12.5 μM.

Isothermal Titration Calorimetry (ITC). The heats of ligand binding to the four duplexes were measured directly by titration calorimetry performed in the TAM 2277 microcalorimeter (Thermometric AB). In each measurement, a duplex solution (2 mL) was titrated at 20 °C with the Net or Dst solution in the same buffer using a motor-driven 250 μL syringe. The ligand concentration was around 0.8 mM, while the DNA concentration in the titration cell was about

Table 2: Binding Constants K_1, K_2, and K ($=K_1K_2$) for Net Binding to the First, Second, and Both Binding Sites of Duplexes D#1−D#4 at 20 °C and the Corresponding Binding Constants K for 2:1 Dst Binding to These Duplexes Determined from UV Melting Curves (T_m°, T_m; Eqs 5 and 6), DSC (ΔH_{hc}), and Titration Calorimetry (ΔH_b) Experiments[a]

duplex	ΔH_{hc}[b] (kcal/mol)	T_m° (°C)	ligand	no. of bound ligands	ΔH_b[b] (kcal/mol)	T_m (°C)	K_1 (M^{-1})	K_2[c] (M^{-1})	K (M^{-2})
			Dst	2	−28.8	56.3			3.5×10^{16}
D#1	95.8	39.0	Net	1	−9.0	54.5	3.1×10^{9}	1.0×10^{6}	
				2	−15.5	56.6			3.1×10^{15}
			Dst	2	−35.4	56.0			1.4×10^{17}
D#2	90.4	37.3	Net	1	−12.5	49.7	9.0×10^{8}	1.8×10^{6}	
				2	−21.3	52.0			1.2×10^{15}
			Dst	2	−28.0	58.0			1.9×10^{16}
D#3	96.1	41.8	Net	1	−10.6	47.8	3.5×10^{7}	2.0×10^{6}	
				2	−18.3	51.0			7.0×10^{13}
			Dst	2	−29.2	58.5			2.4×10^{16}
D#4	96.3	42.6	Net	1	−11.4	48.8	3.7×10^{7}	1.6×10^{6}	
				2	−19.1	51.5			6.0×10^{13}

[a] All values were determined in 10 mM sodium cacodylate, 10 mM NaCl, 1 mM Na_2EDTA buffer solutions; C_{DNA} was 5 μM. [b] ΔH_{hc} and ΔH_b values are expressed per mole of duplex. ΔH_b values for 2:1 Net binding were calculated as the sum of the ΔH_b values of the first and second Net molecules. [c] K_2 values for Net were determined from overall binding constants K and binding constants for binding of the first Net molecule K_1 as $K_2 = K/K_1$.

40 times lower. In a single experiment, 10 injections of 20 μL of the titrant solution were added to the titration cell. The reference cell of the microcalorimeter was filled with the distilled water, and the instrument was calibrated by means of a known electrical pulse. The area under the peak that follows each injection is proportional to the resulting heat of the ligand−DNA interaction. The measured heat effects were around 250 μcal, while the accompanying heats of ligand and DNA dilution were in the order of the experimental error ($\approx$10 μcal) and were neglected. Titration calorimetry was also used for studying the competition between the Net and Dst binding to the 12mer duplexes. In these experiments, Dst−DNA complexes were titrated with Net and vice versa and the accompanying heat effects were followed.

Circular Dichroism (CD) Spectropolarimetry. CD spectra were measured in an AVIV model 62A DS spectropolarimeter (Aviv Associates, Lakewood, NJ) equipped with a thermoelectrically controlled cell holder and a cuvette with a path length of 1 cm. CD titrations were conducted at 20 °C by incrementally injecting 2.5−20 μL aliquots of a Net or Dst solution into 2 mL of a 5 μM duplex solution in the same buffer. The resulting ligand concentration in the DNA−duplex solution increased from 0 to about 20 μM. After each injection, the CD spectrum was recorded between 220 and 400 nm and normalized to a concentration of 1 M. The competition in binding of Dst and Net to the 12mer duplexes was also monitored by CD titrations. In these experiments, each duplex was saturated with one ligand and the resulting 2:1 ligand−DNA complex was titrated with the other ligand and vice versa.

RESULTS AND DISCUSSION

Circular Dichroism

Binding of both drugs to the four duplexes was characterized by measuring the Dst- and Net-induced CD spectra in the wavelength range between 220 and 380 nm. The induced CD signals reflect the ligand−duplex interactions within the ligand−DNA complexes and can therefore be used to monitor the Dst− or Net−DNA binding modes. To see the CD spectral alternations accompanying Dst or Net binding more clearly, the measured CD spectra are presented in the form of difference spectra in which the DNA spectral contributions are subtracted out (Figure 2).

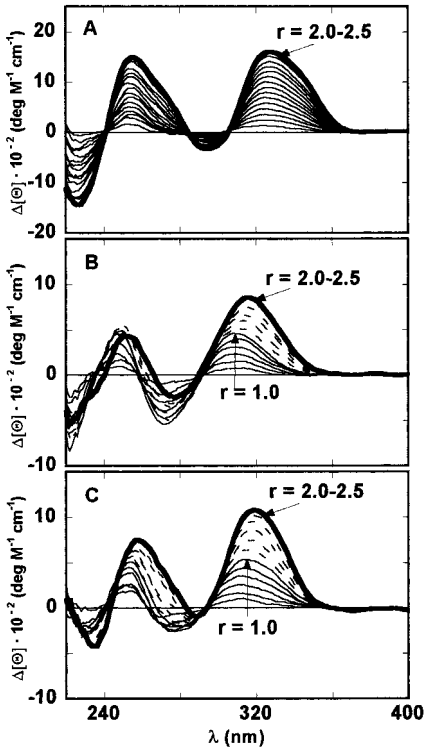

FIGURE 2: Induced CD difference spectra of Dst−D#1 (A), Net−D#2 (B), and Net−D#4 (C) complexes at ligand:duplex ratios, r, varying between 0 and 2.5. T = 20 °C. For Dst binding to D#2−D#4, CD spectra almost identical to those for Dst−D#1 complexes were observed. CD spectra for Net binding to D#1 and D#3 were almost the same as those observed for Net−D#2 and Net−D#4, respectively.

Dst Binding to the Dodecameric Duplexes. As can be seen in Figure 2A, the difference CD spectra of Dst complexes with any of the measured dodecamers show three characteristic isoelliptic points at around 240, 285, and 305 nm, two peaks at 255 and 328 nm, and one minimum at 292 nm. According to the recent CD study of Dst−DNA binding modes by Chen and Sha (*16*), these results indicate an exclusive formation of 2:1 Dst−DNA complexes at all values

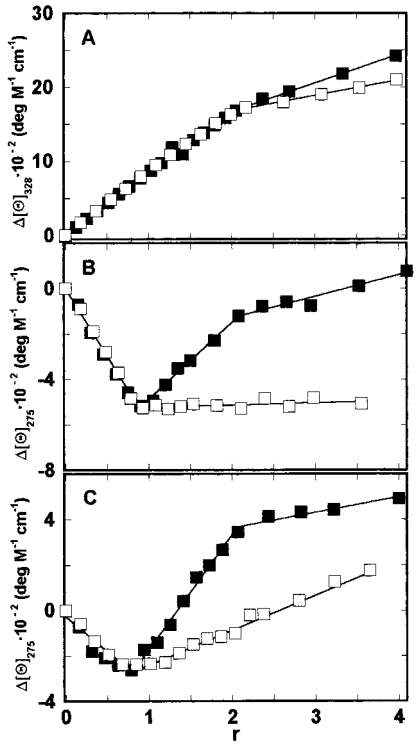

FIGURE 3: CD titration curves presenting the induced ellipticity of Dst−D#1 at 328 nm (A), Net−D#2 at 275 nm (B), and Net−D#4 at 275 nm (C) as a function of the ligand:duplex ratio, *r*, in the presence of 0.1 M NaCl (■) and 0.5 M NaCl (□). $T = 20$ °C.

of the Dst/DNA molar ratio *r* between 0 and 2. The corresponding CD titration curves show that the induced CD peak intensities at 328 nm increase sharply with *r* increasing up to 2, while above 2, this increasing becomes significantly smaller (Figure 3A). The same is also true for the minimum at 292 nm; only the changing of the CD signal between $r = 0$ and 2 is much less pronounced. Our study also shows that when $r \leq 2$ the addition of simple salt has no effect on the slope of the CD titration curves. When $r > 2$, however, this slope is significantly reduced and decreases with increasing salt concentration (Figure 3A). It appears that when $r \leq 2$ the Dst−DNA complexes are stabilized predominantly by the local nonelectrostatic Dst−DNA interactions associated with the deep penetration of Dst into the minor groove, while when $r > 2$, the observed weaker binding of Dst to DNA seems to be governed to a large extent by the electrostatic Dst−DNA interactions occurring at the surface of the duplex molecules.

Sometimes, CD results can provide valuable information about the location of the bound drug within the DNA minor groove. In our study, this was the case with Dst binding to duplex D#1 which besides one five-AT site (5′-TATTT-3′) contains also several potential four-AT·GC binding sites. According to the qualitative ranking for the cooperative binding of the five-AT·GC base pair sites introduced by Chen and Sha (*16*), Dst binds to the 5′-TATTT-3′ site when $r < \sim 0.5$ in a 1:1 mode while its binding to 5′-AAGTT-3′ or 5′-TATAT-3′ sites occurs exclusively in a 2:1 mode. The comparison of these results with our observation that Dst binds to duplex D#1 exclusively in a 2:1 mode (Figures 2A and 3A) leads to a conclusion that Dst binding to D#1 occurs most probably at one of the available four-AT·GC sites and not at the 5′-TATTT-3′ site.

Net Binding to the Dodecameric Duplexes. Net complexes with the four 12mers exhibit distinctly different CD behavior. To duplexes D#1 and D#2 which contain tracts of five successive AT base pairs known to be favorable sites for Net binding within the DNA minor groove Net binds when $r \leq 1$ in a well-defined binding mode. The resulting difference CD spectra are characterized by three isoelliptic points at around 240, 260, and 290 nm, two maxima at 250 and 309 nm, and a minimum at 275 nm (Figure 2B). The salt dependence study reveals that the slopes of the CD titration curves when $r \leq 1$ show almost no dependence on the added salt concentration (Figure 3B). This implies that 1:1 Net−D#1 and Net−D#2 complexes are stabilized primarily by nonelectrostatic interactions. Further binding of Net to D#1 and D#2 when $r > 1$ results in CD spectra that are not complementary to those observed between $r = 0$ and 1 (Figure 2B). Consequently, the CD titration curves measured at properly selected wavelengths abruptly change their slopes when $r = 1$ (at 275 nm even the sign is changed). When $r > 1$, these slopes change very slowly until $r = 2$ where another break point is observed (Figure 3B). At high added salt concentrations, this second break point disappears while the one observed when $r = 1$ remains unaffected. Evidently, a high salt concentration prevents any specific binding of the second Net molecule to the 1:1 Net−D#1 and Net−D#2 complexes. Taken together, these findings suggest that Net binding to duplexes D#1 and D#2 occurs in two distinctive binding modes. The first Net molecule seems to bind to D#1 and D#2 in a high-affinity binding mode determined mainly by the Net−DNA hydrogen bonding and van der Waals interactions for which a deep penetration of Net into the minor groove is required (*5*, *7*). In contrast, the binding of the second Net molecule appears to be of a much lower affinity and strongly governed by the electrostatic Net−DNA interactions. Apparently, the first, strongly bound Net molecule is buried within the minor groove at the five-AT binding site, while the second, weakly bound Net molecule is associated with the D#1 and D#2 surfaces at the unoccupied ends of the duplex molecules. The high- and low-affinity Net-binding sites on the duplex molecules are expected to be separated as much as possible due to the electrostatic repulsion between the two bound ligands.

Analysis of the difference CD spectra of Net complexes with duplexes D#3 and D#4 that contain tracts of only three and two consecutive AT base pairs and the corresponding CD titration curves (Figures 2C and 3C) show that Net also binds to these two dodecamers in two distinctive binding modes. It has to be emphasized, however, that the two different binding modes can be clearly seen only from the CD titration curves observed at the CD minimum at 275 nm and not from those taken at the CD peak intensity at 309 nm where Net binding is usually monitored. As shown in Figure 3C, these CD titration curves are characterized by a clear break point at $r = 1$ where the slope of the titration curve sharply changes its sign and another break point at $r = 2$ where a rather abrupt change of slope is observed. The salt dependence investigation further shows that increasing the simple salt concentration considerably affects only the second break point which at high added salt concentrations completely disappears. These results indicate that Net exhibits different affinities for the two ends of D#3 and D#4 molecules (Figure 1). When $r \leq 1$, the bound Net molecules

appear to be associated with duplex molecules primarily by nonelectrostatic interactions, i.e., by hydrogen bonding and van der Waals contacts, which implies that they are partially buried within the DNA minor groove (probably at the three-AT site). By contrast, further binding of Net to the 1:1 Net−D#3 and Net−D#4 1:1 complexes ($r = 1-2$) appears to be determined predominantly by electrostatic Net−DNA interactions similar to those involved in binding of the second Net molecule to the 1:1 Net−D#1 and Net−D#2 complexes.

Net CD titration curves may be discussed in terms of a simple binding model which assumes that duplex molecules have two independent Net-binding sites, each with its characteristic binding constant K_1 and K_2. The overall binding process can then be described as

$$\begin{aligned} \mathrm{D} + \mathrm{L} &\overset{K_1}{\longleftrightarrow} (\mathrm{DL})_1 \quad K_1 = \frac{[\mathrm{DL}]_1}{[\mathrm{D}][\mathrm{L}]} \\ \mathrm{D} + \mathrm{L} &\overset{K_2}{\longleftrightarrow} (\mathrm{DL})_2 \quad K_2 = \frac{[\mathrm{DL}]_2}{[\mathrm{D}][\mathrm{L}]} \\ \mathrm{D} + 2\mathrm{L} &\overset{K\,(=K_1K_2)}{\longleftrightarrow} \mathrm{DL}_2 \quad K = K_1K_2 = \frac{[\mathrm{DL}_2]}{[\mathrm{D}][\mathrm{L}]^2} \end{aligned} \tag{1}$$

where [D] is the concentration of the free duplex, [L] that of the free ligand, $[DL]_1$ that of the 1:1 Net−DNA complex in which Net is bound at site 1, $[DL]_2$ that of the 1:1 Net−DNA complex in which Net is bound at site 2, and $[DL_2]$ that of the 2:1 Net−DNA complex. The corresponding binding constants are K_1, K_2, and K ($=K_1K_2$). From eq 1, it follows that at any titration point the total added ligand concentration, $[L]_t$, and the total duplex concentration, $[D]_t$, can be presented as

$$[\mathrm{L}]_t = [\mathrm{L}] + (K_1 + K_2)[\mathrm{D}][\mathrm{L}] + 2K_1K_2[\mathrm{D}][\mathrm{L}]^2 \tag{2}$$

$$[\mathrm{D}]_t = [\mathrm{D}] + (K_1 + K_2)[\mathrm{D}][\mathrm{L}] + K_1K_2[\mathrm{D}][\mathrm{L}]^2 \tag{3}$$

Similarly, the corresponding measured difference in molar ellipticity, $\Delta[\theta]_\lambda$, resulting from the bound Net only, can be expressed as

$$\Delta[\theta]_\lambda = A_1[\mathrm{D}][\mathrm{L}] + A_2[\mathrm{D}][\mathrm{L}]^2 \tag{4}$$

where constants A_1 $[(\Delta[\theta_1]_\lambda K_1 + \Delta[\theta_2]_\lambda K_2)/[D]_t]$ and A_2 $(\Delta[\theta_{1,2}]_\lambda K_1K_2/[D]_t)$ are expressed in terms of binding constants K_1 and K_2, the total duplex concentration $[D]_t$, and differences in molar ellipticities $\Delta[\theta_1]_\lambda$, $\Delta[\theta_2]_\lambda$, and $\Delta[\theta_{1,2}]_\lambda$ of complexes $(DL)_1$, $(DL)_2$, and DL_2, respectively. By choosing reasonable values for K_1 and K_2 and solving eqs 2 and 3 for [L] and [D], one can by using the general linear χ^2 fitting procedure (*22*) solve eq 4 for constants A_1 and A_2. By applying the SIMPLEX (*22*) method for the minimization of the χ^2 function with respect to K_1 and K_2, one can finally improve the initial guesses for K_1 and K_2 to obtain the best values for these two fitting parameters. This fitting procedure was applied to the induced CD titration curves constructed for each Net−DNA system at 275, 309, and 320 nm. With the model analysis of these CD titration curves, we obtained at each of the wavelengths approximately the same K_1 and K_2 values; however, the correlations between the adjustable parameters and their variances were the smallest at 275 nm. In other words, the described fitting procedure gives the most reliable estimates of K_1 and K_2 values when performed on CD titration curves measured at 275 nm. In this way, estimated values of K_1 and K_2 presented in Table 1 show that only for duplexes D#1 and D#2 are the K_1 values ($\approx 10^9$ M^{-1}) significantly higher than the corresponding K_2 values ($\approx 10^7$ M^{-1}). This suggests that only to five-AT binding sites does Net bind in a high-affinity binding mode. The other two K_1 values referring to Net binding to D#3 and D#4 and the four K_2 values referring to Net binding to the second binding site of duplexes D#1−D#4 are about the same ($\approx 10^7$ M^{-1}). This is not surprising since they all describe Net binding to sites containing only three or two consecutive AT base pairs. At this point, it has to be mentioned that with the CD titration curves describing Dst binding to the four duplexes a similar fitting procedure based on a highly cooperative 2:1 binding mode cannot be applied since due to extremely high binding constants of Dst ($K \approx 10^{16}$ M^{-2}) the minimization of the χ^2 function results in unacceptably high errors in K.

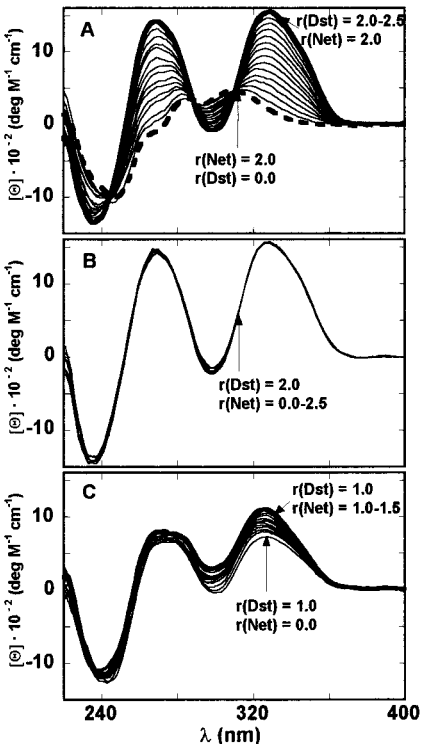

FIGURE 4: CD competition titrations at 20 °C. Titration of the 2:1 Net−D#1 complex with Dst and the resulting CD spectra at Dst:D#1 ratios between 0 and 2.5 (A), CD spectra resulting from the reverse titration of the 2:1 Dst−D#1 complex with Net at Net:D#1 ratios between 0 and 2.5 (B), and CD spectra resulting from the titration of the solution containing Dst and D#1 in a molar ratio of 1:1 with Net at Net:D#1 ratios varying between 0 and 1.5 (C).

Competition Experiments. Competition experiments in which 2:1 Net−DNA complexes were titrated with Dst (Figure 4) clearly show that Dst−DNA complexes are by far dominant forms. According to the observed changes in CD spectra accompanying these titrations, the bound Net molecules are completely displaced by the added Dst molecules which means that the binding affinity of Dst in forming 2:1 Dst−DNA complexes is considerably higher than that of Net in forming the corresponding Net−DNA complexes. This conclusion is further supported by the reverse competition experiments in which titrations of 2:1 Dst−DNA complexes with Net produced no observable

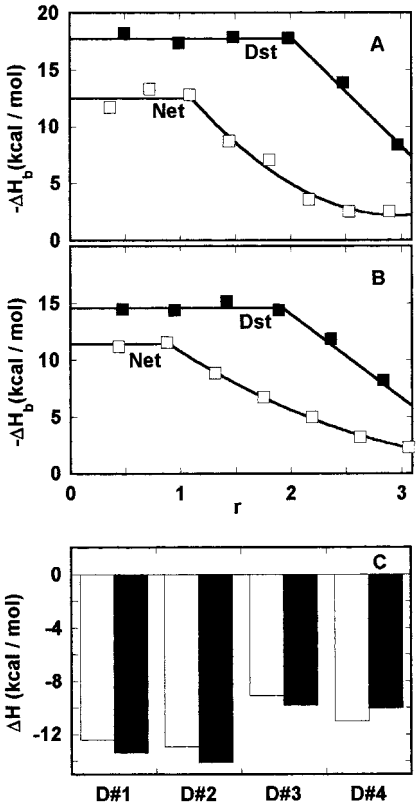

FIGURE 5: Calorimetric binding isotherms (20 °C) of duplexes D#2 (A) and D#4 (B) titrated with Dst (■) and Net (□). ΔH values are expressed in kilocalories per mole of added ligand. Similar calorimetric binding isotherms were obtained also with Dst and Net binding to duplexes D#1 and D#3, respectively. (C) The measured heats of displacement of Net by Dst, ΔH_{ex} (white column), and the corresponding calculated values, ΔH_{calc} (black column), obtained from $\Delta H_{calc} = (\Delta H_b)_{Dst} - (\Delta H_b)_{Net}$, where $(\Delta H_b)_{Dst}$ and $(\Delta H_b)_{Net}$ are the respective enthalpies of Dst and Net binding presented in Table 2.

changes in the measured CD spectra (Figure 4B). If, however, solutions containing Dst and DNA in a 1:1 molar ratio are titrated with Net, the observed spectra are simply the sums of the spectra of the 2:1 Dst−DNA complexes at a concentration equal to one-half of the total DNA concentration and the spectra of the Net−DNA complexes that correspond to a given addition of Net to the other half of the drug-free DNA molecules (Figure 4C). This means that at a Dst:DNA ratio of 1:1 Dst is bound to one-half of the DNA molecules in the form of 2:1 complex while the other half of DNA is drug-free. This observation is consistent with our earlier conclusion based on the CD spectra and CD titration curves that Dst binds to any of the four duplexes exclusively in a dimeric 2:1 mode.

Titration Calorimetry

Dst Binding. Enthalpies of Dst and Net binding to the four duplexes, ΔH_b, measured at the drug:DNA ratios varying between 0 and 3 are presented in Figure 5. Analysis of the heat effects resulting from Dst binding to the four duplexes reveals that when $r \leq 2$ the observed enthalpy of binding to any of the 12mers remains constant. Since Dst spans about five AT·GC base pairs when bound to the DNA duplexes (*15*), the measured dodecamers can provide at most two consecutive binding sites (Figure 1). The question is whether Dst binds predominantly to the two potential binding sites as a monomer or to one site exclusively as a dimer. In the case of monomeric binding, one would expect that due to the different base pair sequences of the two potential binding sites (Figure 1) a noticeable difference in the enthalpy of binding to the first and the second sites would be observed. Since when r is between 0 and 2 the measured ΔH_b values remain constant, one may conclude that when $r \leq 2$ Dst binds to the measured 12mers exclusively in a dimeric 2:1 mode. Such a conclusion is consistent with our CD results as well as with the results of several recent studies on Dst binding to DNA, according to which only sites with sufficiently wide minor grooves can accommodate Dst in a side-by-side manner. Thus, the narrow groove in the 5′-AAAAA-3′ site favors 1:1 binding (*23*, *24*), while a predominantly 2:1 binding is observed when Dst binds within a wider minor groove of the 5′-TATAT-3′ site (*13*) or sites such as 5′-AAGTT-3′ (*17*) and 5′-AAAGT-3′ (*25*) in which a single GC base pair locally widens the minor groove. Inspection of enthalpies of Dst binding to duplexes D#1−D#4 in the 2:1 mode (Table 2) shows that they fall in line with the results of the previously mentioned studies of Dst binding to DNA sites of different geometry and flexibility (*15*, *16*). Thus, for Dst binding to duplex D#1 to which according to our CD results Dst binds to one of its four-AT·GC sites and to duplexes D#3 and D#4 which do contain only four-AT·GC sites, the measured ΔH_b values are almost the same. Such a result seems reasonable since one may expect that a change of the relative base pair positions within the four-AT·GC binding site will not affect significantly the enthalpic contribution to the Dst binding affinity. Binding of Dst to duplex D#2, however, is accompanied by a noticeably more exothermic ΔH_b value. Apparently, the drug−DNA interactions that give rise to the enthalpy-driven binding affinity at the 5′-TATAT-3′ site in D#2, known to be favorable for a dimeric binding of Dst (*13*, *15*), are stronger than those at the four-AT·GC sites in the other three duplexes.

Net Binding. Binding of Net which has been shown to bind preferentially to sites of at least four successive AT base pairs (*5*, *6*, *26*) to any of the measured duplexes is accompanied by a large constant ΔH_b only up to a Net:DNA ratio of 1:1 (Figure 5 and Table 2). When $r < 1$, Net binding to duplexes D#3 and D#4 that contain tracts of at most three consecutive AT base pairs results in almost identical ΔH_b values of about −11 kcal/mol. By contrast, the ΔH_b values accompanying Net binding to 12mers D#1 and D#2 that contain sites of five successive AT base pairs are significantly different. Thus, Net binding to the more "homopolymer-like" 5'-TATTT-3′ site is accompanied by the lowest measured ΔH_b of −9.0 kcal/mol, while its binding to the "heteropolymer-like" 5′-TATAT-3′ site results in the highest exothermic ΔH_b of −12.5 kcal/mol. This large difference in ΔH_b values is similar to the one observed with Net binding to polynucleic acids poly(dA)·poly(dT) and poly(dAT)·poly(dAT) where a much less exothermic ΔH_b value obtained for the homopolymeric poly(dA)·poly(dT) was ascribed to a higher level of hydration of the poly(dA)·poly(dT) minor groove and/or to a lower level of hydration of the Net−poly(dA)·poly(dT) complex (*7*, *27*).

Enthalpies of Net binding to duplexes D#1−D#4 at Net:DNA ratios between 1:1 and 2:1 reflect binding of the second

Net molecule to the available sites on the corresponding 1:1 Net−DNA complexes. Because of the insufficient number of successive AT base pairs at these potential binding sites (Figure 1) and because of the electrostatic repulsion by the Net molecules already bound within the 1:1 complexes, the second Net molecules are expected to bind with lowered affinity. Consequently, the binding constants of the second Net molecule will decrease, causing the corresponding degrees of binding to drop from a value of 1 when $r = 1$ to a value of considerably less than 1 when $r = 2$. Such incomplete binding when r is between 1 and 2 combined with the expected lower enthalpies of Net binding to the potential binding sites on the 1:1 Net−DNA complexes may be considered as the main cause of the observed decreasing of the measured ΔH_b values when r is between 1 and 2. Since when r is between 1 and 2 one cannot distinguish between both contributions to the observed lowering of ΔH_b, the association of the second Net molecule to the 1:1 Net−DNA complexes can be described only in terms of the corresponding average ΔH_b values.

Competition Titrations. Calorimetric competition titrations in which Net−DNA complexes were titrated with Dst and vice versa showed almost no heat exchange when 2:1 Dst−DNA complexes were titrated with Net. In contrast, the reverse titration of 2:1 Net−DNA complexes with Dst resulted in large heat effects, ΔH_{ex}, which are presented in Figure 5C. The measured heats of displacement of Net by Dst are very close to the calculated differences between the overall heats of Dst and Net binding to a given dodecamer, ΔH_{calc} (Figure 5C). This result is consistent with the previously discussed results of the CD competition titrations which have shown that only titrations of Net−DNA complexes with Dst result in substantial changes in the induced CD spectra. Apparently, the overall binding affinity of Dst which binds to the measured dodecamers exclusively in a dimeric, side-by-side manner significantly exceeds that of Net which always binds to these dodecamers as a monomer, either in the 1:1 binding mode (the first Net molecule, five-AT sites with high affinity; three- or two-AT sites with low affinity) or in the 2:1 binding mode (the second Net molecule, only low affinity).

UV Spectrophotometry

Dst Binding. Temperature-induced UV melting curves of the four Dst−DNA complexes measured when r is between 0 and 2.5 show that these complexes behave almost identically. While the ligand-free duplexes melt in monophasic transitions, their Dst complexes at $r \leq 2$ melt in biphasic transitions characterized by two significantly different melting temperatures. When $r \geq 2$, these transitions become again monophasic and occur at the T_m values which are 16−19 °C higher than the T_m values of the corresponding ligand-free duplexes (Figure 6A). The two peaks in the biphasic differential melting curves (Figure 6B) appear for each dodecamer at two specific T_m values which do not depend on the r value. These results strongly suggest that Dst binds to the four dodecamers exclusively in a 2:1 binding mode.

Net binding. Net complexes with the four 12mers show different behavior. When $r = 1$, the bound Net thermally stabilizes duplexes D#1 and D#2 by 15.9 and 12.6 °C and duplexes D#3 and D#4 by only 6.2 and 5.9 °C, respectively.

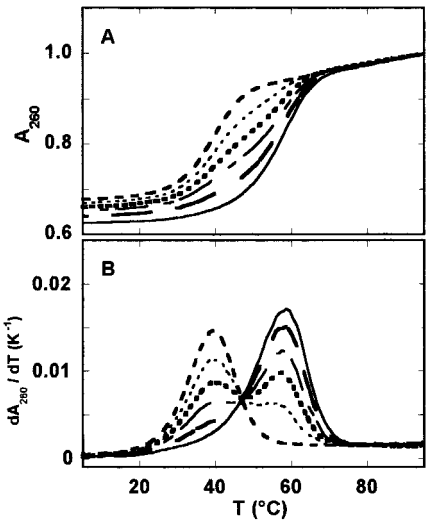

FIGURE 6: UV melting curves of Dst−D#1 complexes at Dst:D#1 ratios of 0 (- - -), 0.4 (···), 0.8 (• • •), 1.2 (- − -), 1.6 (− − −), and 2.0−2.5 (—) (A) and the corresponding differential melting curves (B). Almost identical behavior was observed with Dst−D#2, −D#3, and −D#4 complexes.

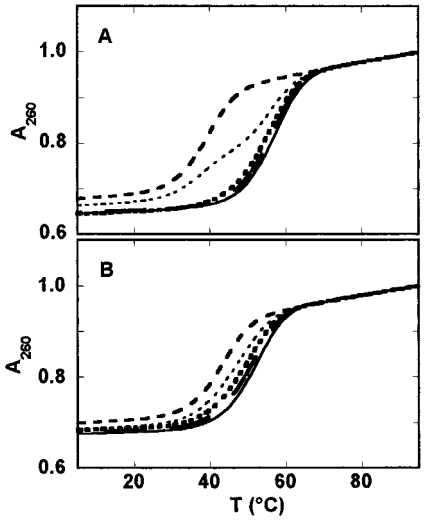

FIGURE 7: UV melting curves of Net−D#1 complexes (A) and Net−D#4 complexes (B) at ligand:duplex ratios of 0 (- - -), 0.5 (···), 1.0 (• • •), 1.5 (− − −), and 2.0−2.5 (—). UV melting curves obtained for Net−D#2 complexes (not shown here) are very similar to those of Net−D#1 complexes, and those determined for Net−D#3 complexes (also not shown here) are almost identical to those of Net−D#4 complexes.

When $r \leq 1$, only Net−D#1 and Net−D#2 complexes exhibit biphasic thermal transitions that seem to be combinations of the thermal transitions of the ligand-free duplexes and their 1:1 Net complexes (Figure 7A). The thermal stabilization of the other two duplexes, D#3 and D#4, is at r between 0 and 1, so low that distinguishing between monophasic and biphasic transitions becomes impossible (Figure 7B). In other words, from these UV melting curves, one cannot make out whether the observed helix to coil transition can be considered as a combination of only the transitions of the ligand-free and ligand-bound 1:1 Net−DNA duplexes. The same problem is encountered with the UV melting curves of the Net complexes with all four duplexes when r is between 1 and 2. They show a further increase in the T_m of about 3 °C. This indicates an additional duplex affinity for the second

Net molecule; however, it gives no information about the type of temperature-induced helix to coil transition of the drug-bound duplex.

Analysis of UV Melting Curves. Our DSC and UV results clearly indicate that the thermally induced helix to coil transitions of all the ligand-free duplexes (DSC), of all the Dst−DNA complexes (UV), and of some of the Net−DNA complexes (UV) occur in a two-state manner. If it is assumed that the helix to coil transitions of Net−D#3 and Net−D#4 complexes when r is between 0 and 1 and of all the Net−DNA complexes when r is between 1 and 2 also occur in a two-state manner, the observed thermal stabilization of duplexes D#1−D#4 induced by the bound Dst or Net can be discussed in terms of the formalism developed by Crothers (*28*). If ligand binding to the single strands is neglected and the ligand−DNA binding stoichiometry is taken into account along with the number of binding sites available per duplex molecule, the measured shifts in the melting temperature, T_m, can be expressed as

$$\frac{1}{T_m^\circ} - \frac{1}{T_m} = \frac{R}{\Delta H_{hc}} \ln(1 + K_{T_m} c_L^{N_h q}) \qquad (5)$$

where T_m° and T_m are the duplex melting temperatures in the absence and presence of the ligand, respectively, ΔH_{hc} is the helix to coil transition enthalpy of the ligand-free duplex, N_h is the number of binding sites per duplex molecule ($N_h = 1$ for Dst and 1 or 2 for Net), q is the number of ligand molecules bound per binding site ($q = 2$ for Dst and 1 for Net), K_{T_m} is the binding constant at T_m ($K = K_1K_2$ for Net when $N_h = 2$), and c_L is half of the total ligand concentration at T_m. For comparative purposes, we extrapolated K_{T_m} values to 20 °C using the van't Hoff relation

$$\ln K_{20°C} = \ln K_{T_m} + \frac{\Delta H_b}{R}\left(\frac{1}{T_m} - \frac{1}{293.15\ \mathrm{K}}\right) \qquad (6)$$

where ΔH_b represents the ligand−DNA binding enthalpy determined at 20 °C by titration calorimetry assumed to be independent of temperature and concentration. As shown by UV melting and differential melting curves, CD spectra and CD titration curves, and calorimetric titrations, Dst appears to bind to each of the four duplexes exclusively in a 2:1 binding mode. Thus, the $K_{20°C}$ values for the formation of 2:1 complexes ($N_h = 1$, $q = 2$) were calculated from eqs 5 and 6 using experimental DSC values for ΔH_{hc}, T_m values determined from the UV melting curves when $r = 2$, and ΔH_b values obtained from the calorimetric titrations (Table 2). Their values are large and very similar ($K \approx 10^{16}$ M^{-2}) which is not surprising since each of the duplexes contains tracts consisting of favorable arrangements of five AT or four AT·GT base pairs (*16*).

Inspection of our UV, CD, and titration calorimetry data referring to Net binding to the four dodecamers reveals that when $r \leq 1$ Net binds to each of the duplexes in a single binding mode. This conclusion is based mainly on the constant enthalpies of binding observed when r is between 0 and 1, on the bound Net-induced CD spectra which show when $r = 1$ several distinct isoelliptic points, and on the CD titration curves which exhibit well-defined break points when $r = 1$. Much sharper break points of CD titration curves when $r = 1$ (Figure 3B,C) and much larger ΔT_m values when $r = 1$ (Figure 7A,B) observed with Net binding to D#1 and D#2 indicate that 1:1 Net binding to these two duplexes is significantly stronger than binding to the other two duplexes. These qualitative conclusions are fully supported by the binding constants K_1 determined for 1:1 Net binding to the four duplexes from eqs 5 and 6 (Table 2). The K_1 values determined for Net binding to duplexes D#1 and D#2 that contain five-AT binding sites are about 2 orders of magnitude higher than those obtained for Net binding to duplexes D#3 and D#4. They are fairly close to K values reported for Net binding to polynucleotides polyd(AT)·polyd(AT) and polyd(A)·polyd(T) (*7*), indicating that Net binding affinity for five-AT binding sites does not depend much on their neighboring base pair arrangements.

Investigation of Net binding to the four 12mers when $r > 1$ shows that due to the small shifts in T_m observed when r is between 1 and 2 the binding constants of the second Net molecule, K_2, can only be estimated from $K_2 = K/K_1$, where K is the total binding constant at $r = 2$ ($N_h = 2$, $q = 1$) and K_1 is the corresponding binding constant of the first Net molecule at $r = 1$ ($N_h = 1$, $q = 1$). Furthermore, the calculation of the K_2 values at 20 °C (Table 2) involves another simplification which may contribute significantly to the overall uncertainty in K_2. Namely, the ΔH_b value when r is between 1 and 2 that has to be used in such calculations can be determined only as an average ΔH_b value over this r range. As already pointed out, close to $r = 2$ the degree of binding of the second Net molecule becomes less than 1, and therefore, such averaging results in an underestimation of the real ΔH_b value. The only way to avoid this difficulty would be to perform calorimetric titration with a sufficient number of points to make an accurate analysis of the measured titration curve possible. Unfortunately, the instrument we were using was not capable of such performance. The values of binding constants K_1 and K_2 characteristic of the first and the second binding mode determined for each dodecamer from eqs 5 and 6 are presented in Table 2. They are in good agreement with the corresponding K_1 and K_2 values estimated by the previously described fitting procedure from the CD titration curves (Table 1). Inspection of Table 2 also shows that 1:1 Net binding to the drug-free duplexes is of significantly higher (D#1 and D#2) and of fairly higher (D#3 and D#4) affinity than the binding of the second Net molecule to the corresponding 1:1 Net−DNA complexes. Furthermore, the K_1K_2 product which is equal to the overall binding constant in the 2:1 Net−DNA complexes is smaller than the corresponding K value for Dst binding in the 2:1 Dst−DNA complexes. This result is fully supported by the previously discussed CD titration and ITC competition experiments which have shown that Dst completely displaces Net from Net−DNA complexes, while upon addition of Net, the Dst−DNA complexes remain unaffected.

Thermodynamics of Dst and Net Binding to the Four Dodecameric Duplexes. The thermodynamic binding profiles for Dst and Net binding to the measured duplexes were determined at 20 °C by combining the general thermodynamic relations $\Delta G_b^\circ = -RT \ln K$ and $\Delta G_b^\circ = \Delta H_b^\circ - T\Delta S_b^\circ$ with the experimental K values obtained from UV melting curves and ΔH_b values obtained from the corresponding calorimetric titrations (Figure 8). In these calculations, it was assumed that ΔH_b does not depend on concentration and therefore may be equated with ΔH_b°. The

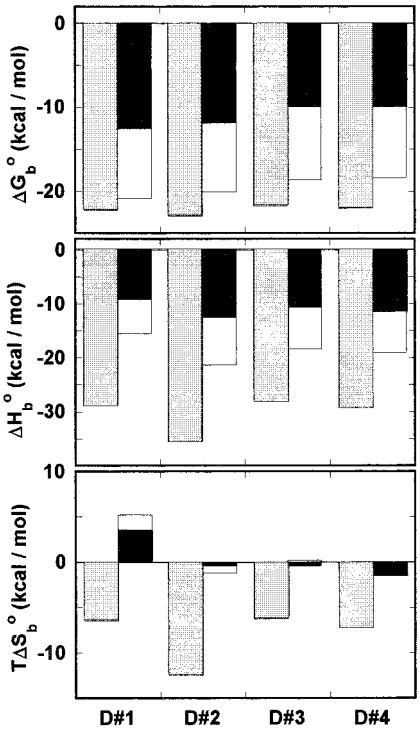

FIGURE 8: Thermodynamic profiles for the dimeric 2:1 binding of Dst (gray column) and successive 1:1 binding of the first Net molecule (black column) and the second Net molecule (white column) to duplexes D#1−D#4 at 20 °C expressed per mole of duplex.

$\Delta G_b°$ values show that the affinity of Dst for formation of 2:1 complexes with any of the duplexes exceeds largely the affinity of Net for formation of 1:1 or 2:1 complexes with the same dodecamers. Inspection of Figure 8 also shows that binding of Dst in the 2:1 mode is a strongly enthalpy-driven process accompanied by a large unfavorable entropy contribution. High exothermic $\Delta H_b°$ values result very likely from local, short-range, nonelectrostatic interactions between Dst and the wall of the minor groove as well as from the additional short-range interactions between the two bound Dst molecules sandwiched within the minor groove in an antiparallel manner. The accompanying large negative $\Delta S_b°$ contributions seem to reflect in the first place the bimolecular association reaction.

As shown in Figure 8, binding of Net to any of the four duplexes is an enthalpy-driven process that is much more sequence-dependent than binding of Dst. The $\Delta G_b°$ values for 1:1 and 2:1 Net binding to duplexes D#1 and D#2 that contain five-AT binding sites are ≈2 kcal/mol more negative than the corresponding $\Delta G_b°$ values for binding to duplexes D#3 and D#4 which contain only tracts of three and two AT consecutive base pairs. Binding of Net to D#2−D#4 is accompanied by entropy contributions that are are small and negative, while binding to D#1 results in $\Delta S_b°$ values that are large and positive. Such behavior can be explained, as previously mentioned in the discussion of the Net−DNA calorimetric titrations, in terms of a higher level of hydration of the D#1 minor groove at the 5′-TATTT-3′ site and/or a lower level of hydration of the Net−D#1 complex. According to this explanation (*7*), Net binding within the D#1 minor groove will result in a larger amount of displaced water molecules accompanied by a greater consumption of energy and increased disorder in the solution (less exothermic $\Delta H_b°$ and more positive $\Delta S_b°$) and/or in a smaller number of water molecules bound to the Net−D#1 complex accompanied by a lower release of energy and less increased order in the solution (less exothermic $\Delta H_b°$ and more positive $\Delta S_b°$).

CONCLUSIONS

We have characterized binding of the minor groove binders Dst and Net to the dodecameric duplexes that contain either one five-AT site and several overlaping four-AT·GC sites (D#1, 5′-TATTT-3′; and D#2, 5′-TATAT-3′) or only three- and two-AT sites and several overlapping four-AT·GC sites (D#3 and D#4). Comparison of our CD results with the CD literature data on the Dst binding to various five-AT and four-AT·GC sites shows that Dst binds to the measured dodecamers exclusively in a 2:1 manner. It further shows that within D#1 which contains the 5′-TATTT-3′ site 2:1 binding of Dst occurs at one of the available four-AT·GC sites rather than at the 5′-TATTT-3′ site. This conclusion is supported by the measured thermodynamic 2:1 binding profiles of Dst which show that for duplexes D#1 (5′-TATTT-3′ site, four-AT·GC sites) and D#3 and D#4 (only four-AT·GC sites) the values of the free energy, enthalpy, and entropy of binding are almost identical, while for duplex D#2 (5′-TATAT-3′ site, four-AT·GC sites), significantly more favorable enthalpy of binding and less favorable entropy of binding are observed. This strongly suggests that Dst binds to D#2 at the 5′-TATAT-3′ site. Exclusive 2:1 binding of Dst to the four duplexes is also confirmed by the measured UV melting curves which show that up to the Dst:DNA ratio of 2:1 only biphasic temperature-induced DNA conformational transitions occur and by the measured enthalpies of binding which remain constant when the Dst:DNA ratio increases from 0 to 2.

In contrast, Net which is known to bind within the DNA minor groove in a 1:1 mode preferentially to sites of at least four successive AT base pairs exhibits high-affinity 1:1 binding ($K_1 \approx 10^9$ M^{-1}) only to duplexes D#1 and D#2 that contain five-AT sites. This indicates that at five-AT sites Net penetrates deep into the minor groove of D#1 or D#2 and makes close contacts with the wall of the minor groove that result in strong van der Waals interactions, hydrogen bonding, and electrostatic interactions. To the other two duplexes that contain tracts of at most three-AT base pairs, Net 1:1 binding is much weaker ($K_1 \approx 10^7$ M^{-1}). The observed independence of the CD titration curves that describe 1:1 binding of Net to D#1−D#4 on the added salt concentration indicates that to duplexes D#3 and D#4 which do not contain sites favorable for Net binding the first Net molecule also binds mainly by nonelectrostatic interactions. This further implies that Net molecules bound to D#3 and D#4 in the form of 1:1 complexes are at least partially buried within the D#3 and D#4 minor grooves. According to our UV and CD results, the second Net molecule binds to any of the four duplexes with almost the same low affinity ($K_2 \approx 10^6$ M^{-1}). The salt dependence of the corresponding CD titration curves reveals that binding of the second Net molecule is governed mainly by the electrostatic Net−DNA interactions that are probably taking place at the surface of the DNA molecules.

Thermodynamic binding profiles describing 2:1 binding of Dst and 1:1 and 2:1 binding of Net to the four duplexes

show that the observed higher binding affinity of Dst is due entirely to its highly exothermic enthalpies of binding. Although the entropies of 2:1 Dst binding are much less favorable than those of Net binding to the same duplexes, the favorable enthalpy contributions for the 2:1 Dst binding prevail and the resulting free energies of Dst binding become significantly more negative. This observation is fully consistent with the results of our CD and calorimetric competition titrations which show that added Dst completely displaces the bound Net from the 2:1 Net−DNA complexes, while the reverse titrations show no displacement effects whatsoever.

Taken together, our results demonstrate that binding of the minor groove binders Dst and Net to DNA depends strongly on the DNA sequence. Parallel spectroscopic and calorimetric studies allow us to distinguish between 2:1 and 1:1 binding modes and to determine the corresponding thermodynamic quantities of binding. Furthermore, these studies also show that from the minor grooves containing sites that favor dimeric 2:1 binding of a given ligand and monomeric 1:1 binding of some other similar ligand the ligand with dimeric 2:1 binding characteristics will almost certainly displace the one that can bind only as a monomeric 1:1 or 2:1 complex.

ACKNOWLEDGMENT

We gratefully acknowledge Prof. Dr. K. J. Breslauer from Rutgers University, The State University of New Jersey (Piscataway, NJ), for providing us with dodecameric strands that were used in this work and for fruitful collaboration in the initial stages of the project. We also thank Prof. Dr. J. Völker from Rutgers University for performing DSC experiments on nano-DSC, for critical reading of the manuscript, and for helpful discussions.

REFERENCES

1. Hahn, F. E. (1977) *Pharmacol. Ther., Part A*, 475−485.
2. Zimmer, C., and Wahnert, U. (1986) *Prog. Biophys. Mol. Biol. 47*, 31−112.
3. Wertell, R. M., Larson, J. E., and Wells, R. E. (1974) *J. Biol. Chem. 249*, 6719−6731.
4. Zimmer, C. (1975) *Prog. Nucleic Acid Res. Mol. Biol. 15*, 285−318.
5. Kopka, M. L., Yoon, C., Goodsell, D., Pjura, P., and Dickerson, R. E. (1985) *Proc. Natl. Acad. Sci. U.S.A. 82*, 1376−1380.
6. Marky, L. A., and Breslauer, K. J. (1987) *Proc. Natl. Acad. Sci. U.S.A. 84*, 4359−4363.
7. Breslauer, K. J., Remeta, D. P., Chou, W.-Y., Ferrante, R., Curry, J., Zaunczkowski, D., Snyder, J. G., and Marky, L. A. (1987) *Proc. Natl. Acad. Sci. U.S.A. 84*, 8922−8926.
8. Breslauer, K. J., Ferrante, R., Marky, L. A., Dervan, P. B., and Youngquist, R. S. (1988) in *Structure & Expression, Volume 2: DNA and Its Drug Complexes* (Sarma, R. H., and Sarma, M. H., Eds.) pp 273−289, Adenine Press, Guilderland, NY.
9. Pelton, J. G., and Wemmer, D. E. (1989) *Proc. Natl. Acad. Sci. U.S.A. 86*, 5723−5727.
10. Pelton, J. G., and Wemmer, D. E. (1990) *J. Am. Chem. Soc. 112*, 1393−1399.
11. Capobianco, M. L., Colonna, F. P., Forni, A., Gabresi, A., Lotti, S., Moretti, I., Samori, B., and Tondelli (1991) *Nucleic Acids Res. 19*, 1695−1698.
12. Dwyer, T. J., Geierstanger, B. H., Bathini, J., Lown, W. J., and Wemmer, D. E. (1992) *J. Am. Chem. Soc. 114*, 5911−5919.
13. Fagen, P., and Wemmer, D. E. (1992) *J. Am. Chem. Soc. 114*, 1080−1081.
14. Rentzeperis, D., and Marky, L. A. (1995) *Biochemistry 34*, 2937−2945.
15. Geierstanger, B. H., and Wemmer, D. E. (1995) *Annu. Rev. Biophys. Biomol. Struct. 24*, 463−493.
16. Chen, F.-M., and Sha, F. (1998) *Biochemistry 37*, 11143−11151.
17. Geierstanger, B. H., Dwyer, T. J., Bathini, Y., Lown, J. W., and Wemmer, D. E. (1993) *J. Am. Chem. Soc. 115*, 4474−4482.
18. *Hamilton HPLC Aplication Handbook* (1993) Hamilton Co., Reno, NV.
19. Griswold, B. L., Hummdler, F. L., and McIntyre, A. R. (1951) *Anal. Chem. 23*, 192−194.
20. Job, P. (1928) *Ann. Chim. (Paris) 9*, 113−134.
21. Marky, L. A., and Breslauer, K. J. (1987) *Biopolymers 26*, 1601−1620.
22. Press, W. H., Flannery, B. P., Teukolsky, S. A., and Vetterling, W. T. (1989) *Numerical Recipies*, Cambridge University Press, Cambridge, U.K.
23. Yoon, C., Privé, G. G., Goodsell, D. S., and Dickerson, R. E. (1988*) Proc. Natl. Acad. Sci. U.S.A. 85*, 6332−6336.
24. Nelson, H. C. H., Finch, J. T., Luisi, B. F., and Klug, F. (1987) *Nature 330*, 221−226.
25. Geierstanger, B. H., Jacobson, J. P., Mrksich, M., Derven, P. B., and Wemmer, D. E. (1994) *Biochemistry 33*, 3055−3062.
26. Patel, D. J. (1982) *Proc. Natl. Acad. Sci. U.S.A. 79*, 6424−6428.
27. Chalikian, T. V., Plum, G. E., Sarvazyan, A. P., and Breslauer, K. J. (1994) *Biochemistry 33*, 8629−8640.
28. Crothers, D. M. (1971) *Biopolymers 10*, 2147−2160.

BI000748U